

Underwater Localization by combining Time-of-Flight and Direction-of-Arrival

Wouter A.P. van Kleunen, Koen C.H. Blom, Nirvana Meratnia,
 André B.J. Kokkeler, Paul J.M. Havinga and Gerard J.M. Smit
 Dep. of Electrical Engineering, Mathematics and Computer Science
 University of Twente, P.O. Box 217, 7500 AE, Enschede, The Netherlands

Abstract—In this paper we present a combined Time-of-Flight (ToF) and Direction-of-Arrival (DoA) localization approach suitable for shallow underwater monitoring applications such as harbor monitoring. Our localization approach combines one-way ranging and DoA estimation to calculate both position and time-synchronization of the blind-node. We will show that using this localization approach, we are able to reduce the number of reference nodes required to perform localization. By combining ToF and DoA, our approach is also capable of tracking and positioning of sound sources under water.

We evaluate our approach through both simulation and underwater experiments in a ten meter deep dive-center (which has many similarities with our target application in terms of depth and reflection). Measurements taken at the dive-center show that this environment is highly reflective and resembles a shallow water harbor environment. Positioning results using the measured Time-of-Arrival (ToA) and DoA indicate that the DoA approach outperforms the ToF approach in our setup. Investigation of the DoA and ToF measurement error distributions, however, indicate the ToF-based localization approach has a higher precision. Shown is that both ToF and DoA and the combined approach achieve sub-meter positional accuracy in the test environment.

Using the error distributions derived from the measurement in the dive-center, we run simulations of the same setup. Results from the simulation indicate ToF is more accurate than DoA positioning. Also in simulation all approaches achieve sub-meter accuracy.

Index Terms—underwater localization, phased arrays, acoustic ranging

I. INTRODUCTION

Accurate localization under water is a challenging task. To estimate the position of a blind node, underwater localization systems use either two-way acoustic ranging between blind and reference nodes or one-way acoustic ranging with synchronous clocks (on both the blind and the reference nodes) [1] [2].

While range-based localization systems use timing information and knowledge about the propagation speed to calculate distance estimates, DoA-based systems use angular information of the incoming signal to determine the position of the blind nodes. In this paper, we focus on one-way ranging with synchronous reference nodes and an asynchronous blind node. Our localization approach combines ToF and DoA information to calculate position and to provide time-synchronization on the blind nodes. Using both ToF and DoA, we are able to reduce the number of reference nodes required to perform localization and will achieve higher localization accuracy. By combining ToF and DoA, our approach is also capable of tracking sound sources and positioning sound sources under water.

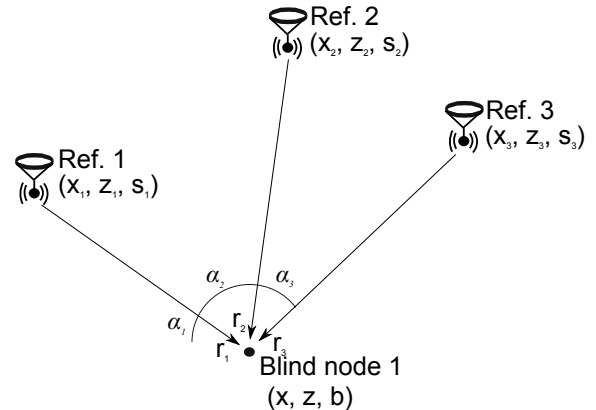


Fig. 1. Example of a DoA and ToF localization: DoA localization uses the angles of incoming signals from reference nodes (α_1 , α_2 and α_3), ToF uses the difference between sending time (s_1 , s_2 and s_3) and receiving time of the signal (r_1 , r_2 and r_3) to estimate the position of the blind node.

The target application of our localization approach is shallow underwater monitoring applications such as monitoring harbor areas, which are located at shallow water reservoirs where many reflections are present. We evaluate our approach through both simulation and underwater experiments in a ten meter deep dive-center (which has many similarities with our target application in terms of deepness and reflection).

The rest of this paper is organized as follows. Section II discusses related underwater time synchronization and localization techniques. In Section III we introduce our ToF, DoA and combined ToF and DoA localization approaches. An overview of the experimental setup at the dive-center and the data acquisition testbed can be found in Section IV. The results of our experimental study are discussed in Section V. Using the error distributions derived from the experimental setup, we run the simulation as presented in Section VI. Finally, in Section VII we summarize the results in our conclusion.

II. RELATED WORK

Figure 1 shows an example of how localization can be performed using DoA or ToF information. Reference nodes send out beacon messages which are received by the blind-node. With DoA localization, the angle of the incoming signal at the blind node is estimated and used to calculate the position of the blind node (x, y) . With ToF localization, the difference between the transmission time of the signal (s_1 , s_2 and s_3) and

reception time (r_1, r_2 and r_3) is recorded and used to calculate both the position (x, z) as well as the clock bias (b) of the blind node. Our work focuses on combining both DoA as well as ToF measurements to calculate the position of the blind node. Note that sound-source localization can be performed by receiving the signal of a blind node at the reference nodes and measuring the reception time and angle at the reference nodes, no changes to the localization approach are required.

Commercial acoustic localization systems, such as Long Baseline (LBL) and Short Baseline (SBL) [3] use two-way ranging between reference nodes and the blind node to estimate the position of the blind-node. A system such as Ultra Short Baseline (USBL) [3] uses two-way ranging between a reference node and a blind node and uses multi-element transducers at the reference node to determine the angle of the incoming signal. Using DoA and ToF information, the position of the blind node can be determined with only a single reference node.

Using two-way ranging increases the amount of communication required and requires cooperation of the blind node. For our application one-way ranging is preferred, because it reduces the amount of communication and allows tracking uncooperating sound sources.

GPS [4] is a well-known ToF localization system that uses one-way ranging to calculate the position and time-synchronization of a blind node. Such an approach can be used in a setup as shown in Figure 1 to calculate the position of the blind node using one-way ranging. ToF localization can be performed by minimizing a Least-Squares form using an iterative optimization technique, such as Levenberg-Marquardt [5].

DoA localization is described in [6], Peng and Sichertiu use a Maximum Likelihood Estimation (MLE) to calculate the most likely position. DoA localization can also be used in a one-way ranging setup as shown in Figure 1.

We consider use of one-way ranging important as it improves the scalability of the localization network. This is due to the fact that the blind nodes do not introduce two-way synchronization overhead. To reduce the number of reference nodes required for the localization and to possibly improve the accuracy of localization, our approach not only uses the ToF acquired through one-way ranging but also the DoA information.

III. UNDERWATER LOCALIZATION

In this section we will introduce our ToF, DoA and combined ToF and DoA localization approaches. We start by introducing the time-synchronization approach and will continue by describing our position estimation approaches.

A. Time synchronization

Time synchronization is the process of synchronizing the clocks of different nodes. This notion of ‘time’ does not necessarily have to be global over all nodes and nodes in the network can agree on a local time for the complete network.

Let us assume that clocks of the reference nodes $i = 1 \dots N$ are denoted by ϕ_i and the clock of an unsynchronized blind node is denoted by ϕ_b . For the ToF measurement we assume

that the reference nodes are synchronized and the blind node has an unknown clock bias denoted by b . For four reference nodes and one blind node, we can write this as the following equation:

$$\phi_1 = \phi_2 = \phi_3 = \phi_4 = \phi_b + b \quad (1)$$

The process of time synchronization is determination of the clock offset b of the blind node. We assume there is no clock-skew and the clock bias is constant. In reality, there is clock-skew. However, because the measurements are taken in a very short time period, we consider the clock-skew to have minimal impact.

B. Localization

To perform localization, ToF and DoA estimates can be used separately or combined. This section describes these three localization methods. We assume that the positions of the four reference nodes are known and the position of reference node i is denoted by (x_i, z_i) . The goal of the localization algorithm is to determine the unknown position of the blind node (x, z) and the unknown clock bias b .

1) *Time-of-Flight based localization*: Given the start time s_i of the reference transmission from TX_i and its measured arrival time r_i at the (unsynchronized) blind node, time synchronization and position estimation can be performed simultaneously. This is done by minimizing the following least-squares estimation:

$$\epsilon_{\text{ToF}} = \min_{(x,z,b)} \sum_{i=1}^N \left(\sqrt{(x-x_i)^2 + (z-z_i)^2} - v \cdot (s_i - b - r_i) \right)^2 \quad (2)$$

Herein, b is the clock bias of the blind node and v is the propagation speed of the signal in water ($\approx 1491\text{m/s}$). The unknown parameters (x, z, b) can be estimated using an iterative optimization approach such as Levenberg-Marquardt [5].

2) *Direction-of-Arrival based localization*: To perform localization based on DoA, we fit the parameters (x, z) to the angles α_i determined by the DoA estimation. To do so, the following equation needs to be minimized:

$$\epsilon_{\text{DoA}} = \min_{(x,z)} \sum_{i=1}^N \left(\tan^{-1} \left(\frac{x-x_i}{z-z_i} \right) - \alpha_i \right)^2 \quad (3)$$

3) *Combined ToF and DoA based localization*: The combined ToF and DoA approach requires minimization of the following equation:

$$\epsilon = \min_{(x,z,b)} (w_{\text{ToF}} \cdot \epsilon_{\text{ToF}} + w_{\text{DoA}} \cdot \epsilon_{\text{DoA}}). \quad (4)$$

For combining the ToF and DoA measurements, weights for the different cost criteria (w_{ToF} and w_{DoA}) need to be determined.

Figure 2 shows the error distribution of the ToF and DoA measurements. The ToF measurements are assumed to be normally distributed $\mathcal{N}(\mu_{\text{ToF}}, \sigma_{\text{ToF}}^2)$. For the distribution of the angular information an extra step is needed to convert it to a positional error. The distribution of the angular information σ_{DoA} can be derived from the measurements, the positional

error distribution can be calculated using the distance d and actually follows the curve shown in Figure 2.

Theoretically, the correct way of calculating the most likely position would be to use a MLE and to model the distribution of the angular error using polar coordinates, as has been done by Peng and Sichitiu [6]. Because our distances and angular errors are small (as this is the case in the harbor monitoring application), we simplify the error model using a straight line rather than a curve. The error distribution of the angular information is modelled as $\mathcal{N}(0, (d \tan(\sigma_{DoA}))^2)$. The error model of the angular information is dependent on the distance estimation d and needs to be updated after every estimation step. Weights for the combined optimization are selected based on the variance of the error distributions of the measurements $w_{ToF} = \frac{1}{\sigma_{ToF}^2}$ and $w_{DoA} = \frac{1}{(d \tan(\sigma_{DoA}))^2}$. Because we use an iterative optimization approach it is straightforward to update these weights after each optimization step.

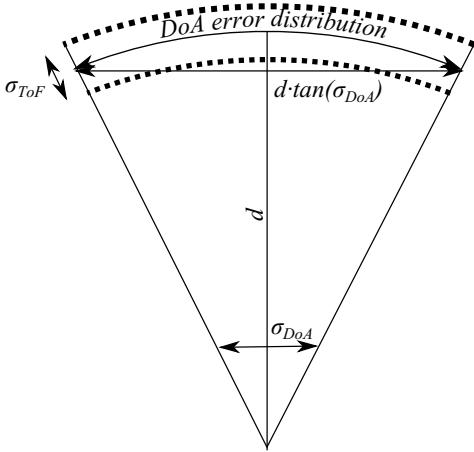


Fig. 2. Error distribution of the ToF and DoA measurement. Positional error of a DoA measurement can be calculated by using the σ_{DoA} and using the (estimated) distance between the blind node and the reference node (d). The positional error is distributed as $\mathcal{N}(0, (d \tan(\sigma_{DoA}))^2)$.

IV. EXPERIMENTAL STUDY

To evaluate the performance of our combined localization approach we have performed underwater experiments in a ten meter deep dive-center. An overview of the setup used in our underwater localization experiment is presented in Section IV-A. The multi-channel underwater testbed being used for data acquisition is described in Section IV-B.

A. Dive-center experiment

During the dive-center experiment, reference transmissions were transmitted sequentially from four transducers attached to a tube floating half a meter below the water surface. At the bottom of the tank, at ten meters of depth, a four-element array captured the reference transmissions. The received signals were recorded using a multi-channel underwater testbed.

Figure 3 shows a technical drawing of the setup, the four reference transducers are denoted by TX₁ to TX₄ with their respective coordinates $(x_1, z_1) \dots (x_4, z_4)$. The goal of the

localization algorithm is to determine the unknown location (x, z) of the array at the bottom of the tank. In terms of Underwater Acoustic Sensor Networks (UASNs), the reference transducers can be considered as reference nodes and the array as blind node.

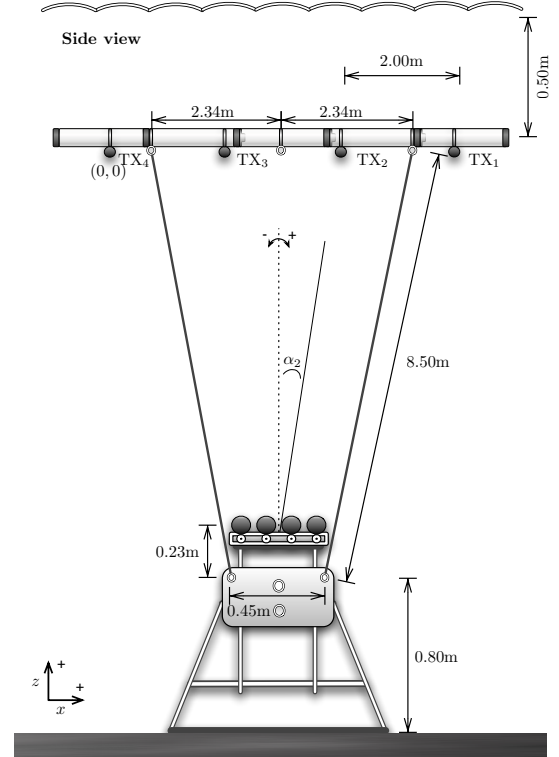


Fig. 3. Technical drawing of dive-center setup (not to scale).

Figure 4 shows a segmented panorama of the actual test setup in the dive-center.

B. Low-cost Multi-channel Testbed

The multi-channel acoustic signal processing testbed described in [7] has been used to capture the signals of the four-element array. The testbed consists of an off-the-shelf FPGA board and an easy to build (data-acquisition) extension board. A simplified schematic of the testbed is shown in Figure 5. Underwater acoustic pressure waves are converted to voltages by the four piezoelectric transducers of the array. After amplification and filtering, all analog signals are synchronously sampled and copied to the on-board memory of the FPGA board. After each experiment, raw sample data was copied from the on-board SDRAM to a PC for offline post-processing.

C. Methodology

The reference transmissions are frequency sweeps from 20kHz to 40kHz. Each sweep has a duration of 90ms and is followed by 10ms of silence. After each sweep the active transducer is switched.

Based on the multi-channel recording of the array, the ToF and the DoA of a reference transmission can be determined.

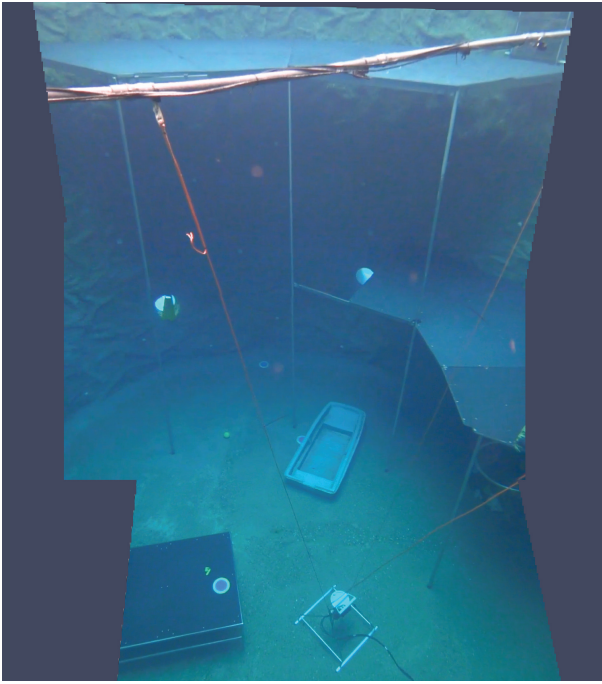


Fig. 4. Segmented panorama of the dive-center setup.

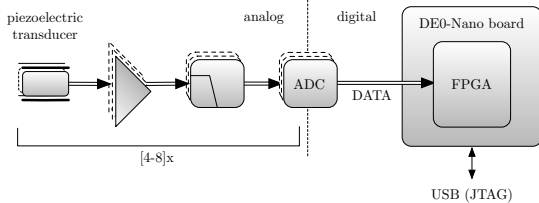


Fig. 5. Overview of the multi-channel underwater testbed.

The ToF is found by cross-correlation of the received signals and the reference signals. A linear beamscan, in the 20kHz to 22kHz subband, is used to find the DoA of an incoming reference transmission.

D. Acoustic Ranging

The acoustic range is a distance estimate based on the ToF and the acoustic propagation speed v in the medium. To determine an estimate of the ToF an approximation of the arrival time of the reference signal is required. The (discrete-time normalized) cross-correlation $c_{sr}[l]$ of the reference signal s can be used to accurately determine the arrival time of the reference signal:

$$c_{sr}[l] = \frac{1}{\sqrt{c_{ss}[0]c_{rr}[0]}} \cdot \sum_{n=1}^{N-l} s[n]r[n+l], \quad l \geq 0. \quad (5)$$

Herein, l is the lag parameter, N is the number of samples of the input sequences and $c_{ss}[0]$ and $c_{rr}[0]$ are the mean-square signal powers of s and r . The lag time of the Line-of-Sight (LoS) arrival, in terms of samples, can be found by application of a simple threshold on the baseband representation of the cross-correlation results. We assume that the first peak having

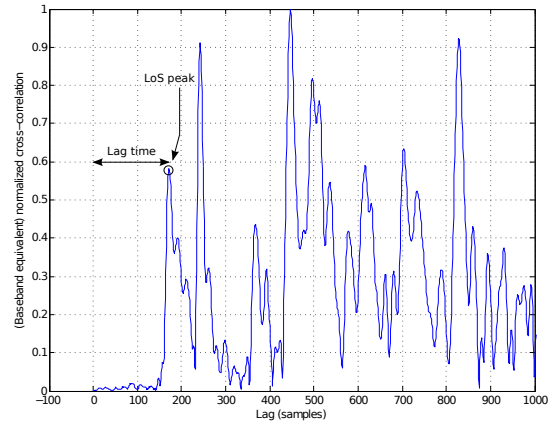


Fig. 6. Cross-correlation results of acoustic reference sweep.

a correlation of at least 50% of the maximum correlation represents the LoS path.

Given the sample frequency of s and r , the lag time of the LoS arrival is rounded to find an estimate of the arrival time.

E. Direction-of-Arrival Estimation

The four-element transducer array is used to estimate the DoA angle of a reference transmission. In our experiment, the acoustic bandwidth of the sweep signal is in the order of its carrier frequency. Decomposing this wideband sweep into multiple ‘narrow’ subbands validates the use of narrowband beamforming to create directivity [8]. Narrowband beamforming (based on phase shifts) in the 20-22 kHz subband has been used to determine the signal power in a certain direction. A linear scan over all broadside look angles is performed to determine the signal power for every angle. The latter is known as the spatial spectrum. The angle corresponding to the strongest signal power is considered the actual LoS arrival angle.

V. EXPERIMENTAL RESULTS

A typical cross-correlation and lag time from a received underwater transmission in the test environment is shown in Figure 6. What can be seen from this cross-correlation is that many multi-path signals are present in the environment. Moreover some of the multi-path signals were received stronger than the LoS signal. These are the same difficult conditions attributed to shallow water and high reflection that we expect to face for shallow harbor monitoring. Successful and accurate localization in such environment can also guarantee the accuracy and success of our approach for harbor monitoring.

Figure 7 shows the results of the spatial spectra for four reference transmissions. Based on the linear beam scan, we found the mean DoA angles of the reference transducers (TX₄...TX₁) to be -17.9 , -3.86 , 10.66 and 20.86 degrees.

Using the measurements we have determined the error distribution for ToF to be $\sigma_{ToF} = 0.1219 \cdot 10^{-5}m$. For the DoA the error distribution of the measured angles is $\sigma_{DoA} = 0.1817^\circ, 0.1140^\circ, 0.0548^\circ, 0.0548^\circ$. If we use the knowledge that the distance between the array and the

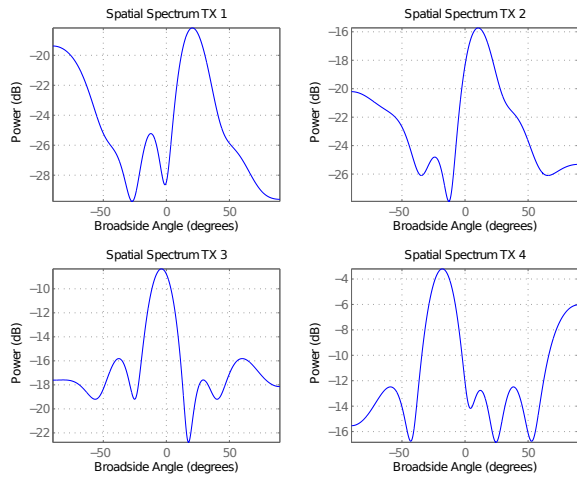


Fig. 7. Measured spatial spectra.

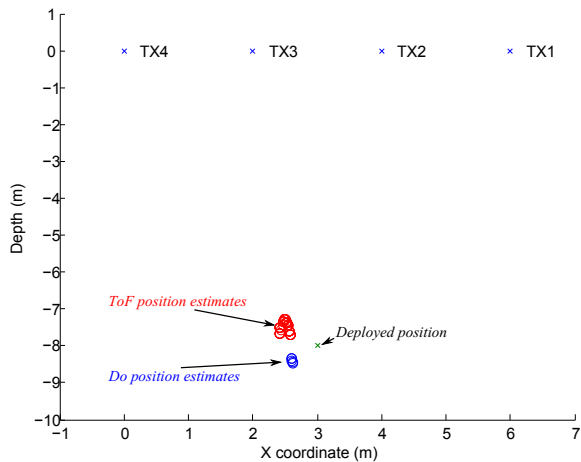


Fig. 8. Result DoA and ToF-based localization. ToF underestimates the depth of the array and places the positions above the array, DoA overestimates the depth of the array and places the positions under the array. Results indicate an average position error of 71cm for ToF and 56cm for DoA positioning.

beacons is about 8.3514 meters, the error distribution of the angular localization is approximately $d \cdot \tan(\sigma_{DoA}) = 2.65 \cdot 10^{-2}m, 1.66 \cdot 10^{-2}m, 0.80 \cdot 10^{-2}m, 0.80 \cdot 10^{-2}m$. Using this information we can conclude that according to these measurement the ToF measurement is more accurate than the DoA measurement.

Figure IV-A shows that the center of the array is, in theory, positioned at $(x = 3.00, y = -8.05)$. Based on ToF estimates for the reference transmissions, the position of the array is estimated. The results of ToF-based localization (for forty-eight distinct measurements) and the DoA-based localization (for twelve measurements) are shown in Figure 8.

Results of both localization methods indicate that the array was located to the left of the calculated deployment position. When we look at the distance between the ToF calculated positions and the deployed position of the array, we can see that the calculated ToF position is placed on average 71cm from the deployed position of the array. The calculated positions from the DoA position are placed 56cm from the deployed

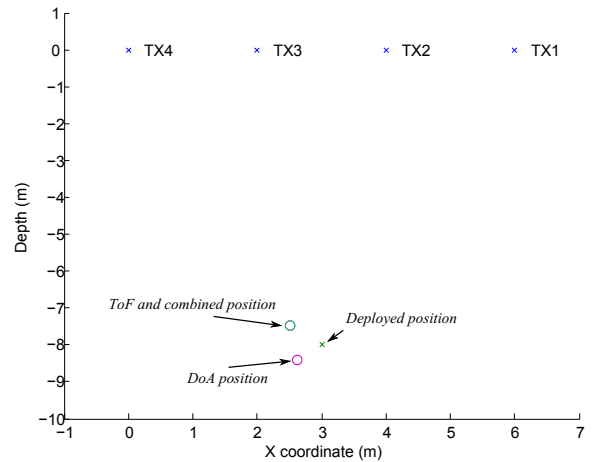


Fig. 9. DoA, ToF and combined localization. Calculated position for ToF and combined ToF and DoA is $(2.51, -7.49)$, calculated position for DoA localization is $(2.61, -8.40)$. The position of the array is $(3.00, -8.05)$.

position of the array.

The error distribution of the ToF position is $\mathcal{N}(0.71, 0.12)$. The error distribution of the calculated positions for DoA is $\mathcal{N}(0.56, 0.03)$. This indicates that in this setup the DoA position calculation is more accurate than the ToF position.

We tried to position the array centered underneath the tube with reference transducers. However, this task turned out to be fairly difficult under water. A slight mis-alignment was visually observed during the experiment and the array was indeed actually more positioned to the left. Therefore, in reality the calculated positions were actually more accurate than the 71cm and 56cm originally calculated. This is in contradiction with results we have obtained before, so we cannot conclude whether the DoA or ToF approach is the most accurate. From these results we can conclude, however, that both methods achieve sub-meter accuracy. Note that ToF-based localization seems to underestimate the actual depth while DoA-based localization overestimates the depth. An explanation of the conflicting results may be that the actual depth of the array was different (shallower) than where we tried to position the array.

Results for combined ToF and DoA localization can be seen in Figure 9. The combined localization approach pulls completely to the ToF result. This is the result of the measured σ_{ToF} and σ_{DoA} . The standard deviation of the ToF error distribution is significantly smaller than the standard deviation of the DoA distribution, weights for the ToF measurement are orders of magnitude larger than the DoA weights.

VI. SIMULATION RESULTS

Using simulations we will show the expected performance of our combined ToF and DoA localization approach in a more controlled setup. To perform simulation use the ToF and DoA error that we derived from the experimental setup.

In the simulations we use the same setup as the experimental setup. The 4 reference nodes are placed at the surface and the blind node is placed at the same position as in the experimental

setup. Rather than performing measurements, we use the derived error distributions from the experiment to simulate measurements errors. We run the simulation for 100 different measurements, the results are shown in Figure 10.

	μ	σ
ToF $\mathcal{N}(0.0, 0.1219 \cdot 10^{-5})$	0.0522m	$1.8391 \cdot 10^{-4}m$
DoA $\mathcal{N}(0.0, 1.4775 \cdot 10^{-2})$	0.4174m	0.3157m
Combined	0.0522m	$1.8391 \cdot 10^{-4}m$

Fig. 10. Simulated calibration accuracy, ToF, DoA and combined ToF and DoA are performed in a simulated deployment similar to the setup of the experiment. Shown are the average positional error and standard deviation of the error.

Similar results as from the experiment can be seen in the simulation, the result of the combined solutions pull toward the ToF result. This is the result of the large difference in measured error distributions of the measurements. The ToF is weighted more significant because of the small error deviation. Different from the experimental results, the ToF is more accurate than the DoA positioning. We think that in the experimental setup the ToF is also actually more accurate than the DoA result, and the position of the array is actually positioned more towards the ToF calculated position. Similar to the experiments, the simulation achieves sub-meter accuracy for all localization approaches.

VII. CONCLUSION

We consider one-way ranging important for localization under water because it improves the energy-efficiency and scalability. Both ToF and DoA localization can estimate a position using one-way ranging only. By combining ToF and DoA, the number of reference node required to perform localization can be reduced. Therefore in this work we propose a combined ToF and DoA localization approach.

The goal of our localization approach is to provide localization and sound-source tracking in short-range shallow water environments such as a harbor. These environments are highly reflective and may contain many multi-path signals. To simulate such an environment the experiments were performed in a dive-center. ToF measurements were performed by measuring the propagation time of transmissions between moored reference transducers and a transducer array at the bottom of the tank. The DoA measurement was performed by determining the DoA angle of the signal impinging on the transducer array. The cross-correlation of the received signal shows that the environment is indeed a highly reflective environment.

Looking at the results of the position calculation, we conclude that in our setup DoA outperforms ToF localization. However looking at the error distribution of the measurements, the angular measurements show a greater deviation than the ToF measurements, indicating the ToF localization to be more precise. What we can conclude is that both approaches and the combined localization approach achieve sub-meter accuracy.

We have used the error distributions derived from the experiment to perform simulations. From the simulations it becomes clear the ToF performs better than DoA positioning. The

conflicting results of the experimental setup (DoA performing better than ToF) are likely the cause of a misplacement of the array. Similar to the experimental results, the position of the combined approach in the simulation pull completely towards the ToF calculated result. This is a result of the big difference in the deviation of the error distributions of DoA and ToF measurement. In simulation again, all approaches achieve sub-meter accuracy.

Future work will include similar measurements over larger distances in a more dynamic environment, e.g. a lake or a harbor. In the setup we would like to more accurately determine the position of the array. We attempted to position the array directly under the middle of the transmitters line, however this proved to be very difficult and a positioning error could be visually observed during the test.

ACKNOWLEDGMENT

The work presented in this paper is supported by the STW project: SeaSTAR (10552). The authors would like to thank Kenneth Rovers and Niels Moseley for their help during the experiment.

REFERENCES

- [1] R. Eustice, L. Whitcomb, H. Singh, and M. Grund, "Experimental results in synchronous-clock one-way-travel-time acoustic navigation for autonomous underwater vehicles," in *Robotics and Automation, 2007 IEEE International Conference on*. IEEE, 2007, pp. 4257–4264.
- [2] P. Miller, J. Farrell, Y. Zhao, and V. Djapic, "Autonomous underwater vehicle navigation," *Oceanic Engineering, IEEE Journal of*, vol. 35, no. 3, pp. 663–678, 2010.
- [3] K. Vickery, "Acoustic positioning systems: a practical overview of current systems," in *Autonomous Underwater Vehicles, 1998. AUV'98. Proceedings of the 1998 Workshop on*, aug 1998, pp. 5–17.
- [4] B. W. Parkinson, A. I. for Aeronautics, Astronautics, GPS, and NAVSTAR, *Global positioning systems : theory and applications. Vol. 2*. American Institute of Aeronautics and Astronautics, 1996.
- [5] J. J. Moré, "The levenberg-marquardt algorithm: Implementation and theory," in *Numerical Analysis*, ser. Lecture Notes in Mathematics, G. Watson, Ed. Springer Berlin Heidelberg, 1978, vol. 630, pp. 105–116.
- [6] R. Peng and M. L. Sichitiu, "Angle of arrival localization for wireless sensor networks," in *SECON*. IEEE, 2006, pp. 374–382.
- [7] K. Blom, R. Wester, A. Kokkeler, and G. Smit, "Low-cost multi-channel underwater acoustic signal processing testbed," in *The Seventh IEEE Sensor Array and Multichannel Signal Processing Workshop*, 2012.
- [8] W. Liu and S. Weiss, *Wideband Beamforming*, X. Shen and Y. Pan, Eds. Wiley, 2010.